

AD-A174 882

THE IDENTIFICATION OF A DISTRIBUTED PARAMETER MODEL FOR
A FLEXIBLE STRUCT. (U) BROWN UNIV PROVIDENCE RI
LEFSCHETZ CENTER FOR DYNAMICAL SYSTE..

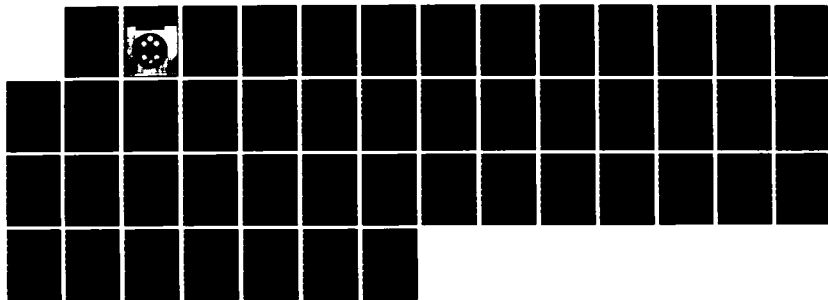
1/1

UNCLASSIFIED

H T BANKS ET AL. AUG 86 LCDS-86-32

F/G 13/13

NL





NATIONAL BUREAU OF STANDARDS
 RESOLUTION TEST CHART
 1963-A-10

AD-A174 802

DISTRIBUTION STATEMENT A

Approved for public release;
Distribution Unlimited

**THE IDENTIFICATION OF A DISTRIBUTED
PARAMETER MODEL FOR A FLEXIBLE STRUCTURE**

by

H.T. Banks, S.S. Gates, I.G. Rosen, Y. Wang

August 1986

LCDS #86-32

DTIC
CTE

DEC 4 1986

B

Approved
distribution

Lefschetz Center for Dynamical Systems

DTIC FILE COPY

**THE IDENTIFICATION OF A DISTRIBUTED
PARAMETER MODEL FOR A FLEXIBLE STRUCTURE**

by

H.T. Banks, S.S. Gates, I.G. Rosen, Y. Wang

August 1986

LCDS #86-32

DTIC
ELECTE
DEC 4 1986

E

UNCLASSIFIED DOCUMENT A
Approved for public release;
Distribution unlimited

UNCLASSIFIED

SECURITY CLASSIFICATION OF THIS PAGE (When Data Entered)

REPORT DOCUMENTATION PAGE		READ INSTRUCTIONS BEFORE COMPLETING FORM
1. REPORT NUMBER AFOSR-TR- 86-2034	2. GOVT ACCESSION NO.	3. RECIPIENT'S CATALOG NUMBER
4. TITLE (and Subtitle) The Identification of a Distributed Parameter Model for a Flexible Structure		5. TYPE OF REPORT & PERIOD COVERED Reprint
7. AUTHOR(s) H.T. Banks, S.S. Gates, I.G. Rosen, Y. Wang		6. PERFORMING ORG. REPORT NUMBER
9. PERFORMING ORGANIZATION NAME AND ADDRESS Lefschetz Center for Dynamical Systems Division of Applied Mathematics Brown University, Providence, RI 02912		8. CONTRACT OR GRANT NUMBER(s) AFOSR 84-0393
11. CONTROLLING OFFICE NAME AND ADDRESS Air Force Office of Scientific Research Bolling Air Force Base Washington, DC 20332 nm		10. PROGRAM ELEMENT, PROJECT, TASK AREA & WORK UNIT NUMBERS 61102 F 2304/A1
14. MONITORING AGENCY NAME & ADDRESS (if different from Controlling Office) Same as 11		12. REPORT DATE August 1986
		13. NUMBER OF PAGES 41
		15. SECURITY CLASS. (of this report) Unclassified
		15a. DECLASSIFICATION/DOWNGRADING SCHEDULE
16. DISTRIBUTION STATEMENT (of this Report) Approved for public release: distribution unlimited		
17. DISTRIBUTION STATEMENT (of the abstract entered in Block 20, if different from Report) Approved for public release; distribution unlimited.		
18. SUPPLEMENTARY NOTES		
19. KEY WORDS (Continue on reverse side if necessary and identify by block number)		
20. ABSTRACT (Continue on reverse side if necessary and identify by block number) INCLUDED		

DD FORM 1 JAN 73 1473

EDITION OF 1 NOV 65 IS OBSOLETE
S/N 0102-LF-014-6601

UNCLASSIFIED

SECURITY CLASSIFICATION OF THIS PAGE (When Data Entered)

THE IDENTIFICATION OF A DISTRIBUTED PARAMETER MODEL
FOR A FLEXIBLE STRUCTURE

H. T. Banks^{1,3}
Lefschetz Center for Dynamical Systems
Div. of Applied Mathematics
Brown University
Providence, RI 02912

S. S. Gates
The Charles Stark Draper Laboratory, Inc.
Cambridge, MA 02139

I. G. Rosen^{2,3}
Dept. of Mathematics
University of Southern California
Los Angeles, CA 90089

Y. Wang²
Dept. of Mathematics
University of Southern California
Los Angeles, CA 90089

(1) This research was supported in part by the National Science Foundation under NSF Grant MCS-8504316, the Air Force Office of Scientific Research under Contract AFOSR-84-0398, and the National Aeronautics and Space Administration under NASA Grant NAG-1-517.

(2) This research was supported in part by the Air Force Office of Scientific Research under Contract AFOSR-84-0393.

(3) Part of this research was carried out while these authors were visiting scientists at the Institute for Computer Applications in Science and Engineering (ICASE), NASA Langley Research Center, Hampton, VA, which is operated under NASA Contracts NAS1-17070 and NAS1-18107

ABSTRACT

We develop a computational method for the estimation of parameters in a distributed model for a flexible structure. The structure we consider (part of the "RPL experiment") consists of a cantilevered beam with a thruster and linear accelerometer at the free end. The thruster is fed by a pressurized hose whose horizontal motion effects the transverse vibration of the beam. We use the Euler-Bernoulli theory to model the vibration of the beam and treat the hose-thruster assembly as a lumped or point mass-dashpot-spring system at the tip. Using measurements of linear acceleration at the tip, we estimate the hose parameters (mass, stiffness, damping) and a Voigt-Kelvin viscoelastic structural damping parameter for the beam using a least squares fit to the data.

We consider spline based approximations to the hybrid (coupled ordinary and partial differential equations) system; theoretical convergence results and numerical studies with both simulation and actual experimental data obtained from the structure are presented and discussed.

Accession For	
NTIS	✓
DTIC	
AD	



A-1

1. Introduction

The difficulties involved in the design of practical and efficient control laws for large flexible spacecraft (e.g. the inherent infinite dimensionality of the system, a large number of closely spaced modal frequencies, high flexibility, light damping, a fuel-limited, hostile, highly variable environment, etc.) have stimulated research into the development of system identification and parameter estimation procedures which will yield high fidelity models. A particular area of interest involves schemes for the estimation of material parameters describing, for example, mass, inertia, stiffness or damping properties in distributed models for the vibration of viscoelastic systems—specifically, mechanical beams, plates and the like. In addition, since the resulting inverse problems are often infinite dimensional, substantial attention has been focused on approximation; see, for example, [1], [2], [3], [4], [8] and [12]. In these treatments, the parameter estimation problem is formulated as a least squares fit to measurements of either displacement or velocity. Although significant gains have been made in the development of instrumentation to measure displacement and velocity (e.g. laser technology, etc.), one of the least expensive, most reliable and most commonly used sensors is the linear accelerometer. While in principle it is possible to integrate acceleration measurements once or twice to obtain respectively velocity or displacement data, in practice this task can pose significant challenges. For example, integration of the signal could result in the amplification of low frequency measurement noise or dynamic effects which have not been included in the underlying model. In light of this, we have undertaken to show here, both

theoretically and computationally, that a scheme in the spirit of those developed in the previously cited references can also be effectively used with acceleration measurements. In particular we note, this involves the nontrivial extension of the familiar variational arguments which are used to demonstrate the convergence of the finite element state approximations upon which the identification schemes are based. Indeed, it must be shown that in addition to the convergence of the displacement and velocity, the convergence of acceleration can be obtained as well.

The other primary motivation for the present effort is that while these methods have been extensively tested and evaluated with simulation data, they have never been tried with actual experimental data. We have tested our scheme with data obtained from an experimental structure which was designed and constructed at the Charles Stark Draper Laboratory in Cambridge, Massachusetts with funding provided by the United States Air Force Rocket Propulsion Laboratory (RPL). The RPL structure (as it will henceforth be referred to as) was designed to serve as a test bed for the implementation and evaluation of control algorithms for large angle slewing of spacecraft with flexible appendages. The structure was specifically designed to exhibit structural modes and damping characteristics representative of realistic large flexible space structures.

In Section 2 we describe the RPL structure (its geometry, instrumentation, etc.) and formulate an inverse problem involving a distributed system. In Section 3, we use the resulting infinite dimensional estimation problem to motivate the development of a finite dimensional, finite element based approximation scheme. We also

discuss our theoretical convergence results. In Section 4 we present numerical findings.

We use standard notation throughout. For X a normed linear space, $L(X)$ denotes the space of bounded linear operators from X into X . For Ω an interval and $k = 0, 1, 2, \dots$, $C^k(\Omega; X)$ denotes the space of functions from Ω into X which are k times continuously strongly differentiable on Ω . When $k = 0$ we shall simply write $C(\Omega; X)$. A function f from Ω into X will be said to belong to $L_2(\Omega; X)$ if $\int_{\Omega} |f(t)|_X^2 dt < \infty$. For $k = 0, 1, 2, \dots$, $H^k(\Omega; X)$ denotes the completion of $C^k(\Omega; X)$ with respect to the norm

$$|f|_k = \left(\sum_{j=0}^k \int_{\Omega} |f^{(j)}(t)|_X^2 dt \right)^{1/2}.$$

If, in addition, X is a Hilbert space with inner product $\langle \cdot, \cdot \rangle_X$ then $H^k(\Omega; X)$ is a Hilbert space with inner product

$$\langle f, g \rangle_k = \sum_{j=0}^k \int_{\Omega} \langle f^{(j)}(t), g^{(j)}(t) \rangle_X dt.$$

When $X = \mathbb{R}$, we use the abbreviated notations $C^k(\Omega)$, $L_2(\Omega)$ and $H^k(\Omega)$. Note that $H^0(\Omega) = L_2(\Omega)$ and $\langle \cdot, \cdot \rangle_0$ is the standard inner product on $L_2(\Omega)$.

2. The Identification Problem

The RPL structure (see Figure 2.1 below) consists of four flexible appendages which are cantilevered at right angles to one another from a rigid central hub. The hub is mounted on an air bearing table thus permitting the near frictionless rotation of the structure about the vertical axis.

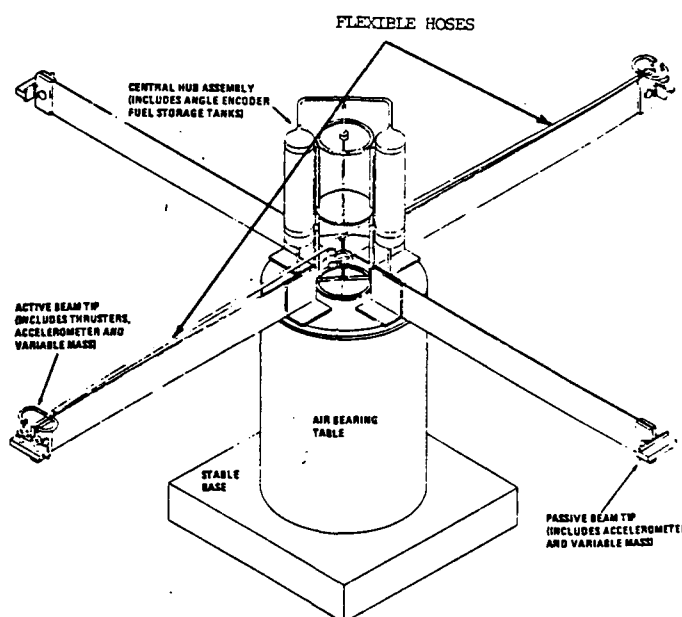


Figure 2.1

Two of the appendages (which are mounted to the hub 180° apart) are "active"; each has two nitrogen cold gas thrusters mounted in opposing directions at its tip. The remaining two appendages are "passive" with only counter-balancing masses affixed to their free ends. The presence of the tip masses on the passive arms serves to preserve the

overall symmetry of the structure. Nitrogen gas from tanks mounted on the central hub is supplied to the thrusters via two stainless steel mesh-wrapped high pressure hoses. The expulsion of propellant from the thruster nozzles is controlled by electro-mechanical or solenoidal valves. Each of the four appendages is equipped with a sensor in the form of a linear accelerometer attached at its tip. Data from the accelerometers is processed and recorded and control input signals to the thrusters are generated by a MINC 11/23 microcomputer. A detailed description of the structure's design specifications can be found in [6] and [15].

The problem which is of primary concern to us here involves the modeling of the effects of the nitrogen supply hoses on the transverse vibration of the active members. We consider therefore, the structure with the central hub immobilized and look only at the vibration of one of the active appendages and view it as a simple cantilevered beam (see Figure 2.2).

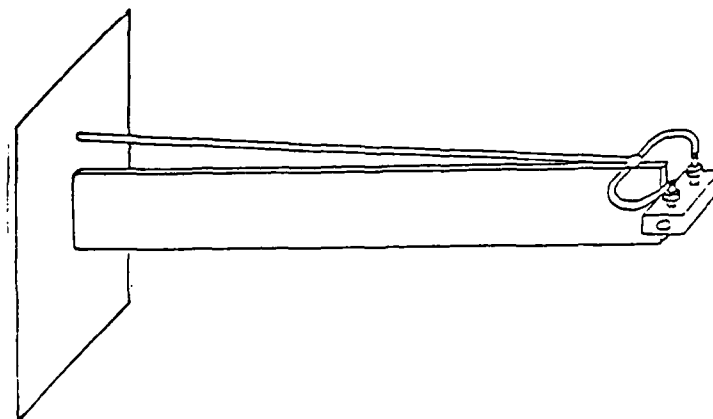


Figure 2.2

We treat the thruster assembly as a point mass that is rigidly attached to the beam at the tip and propose a model for the hose effects in the form of a proof mass which reacts against the tip mass. In effect, we consider the idealized, simplified structure depicted in Figure 2.3 below involving a single, cantilevered, flexible, uniform beam with a two-mass-dashpot-spring system affixed to its free end.

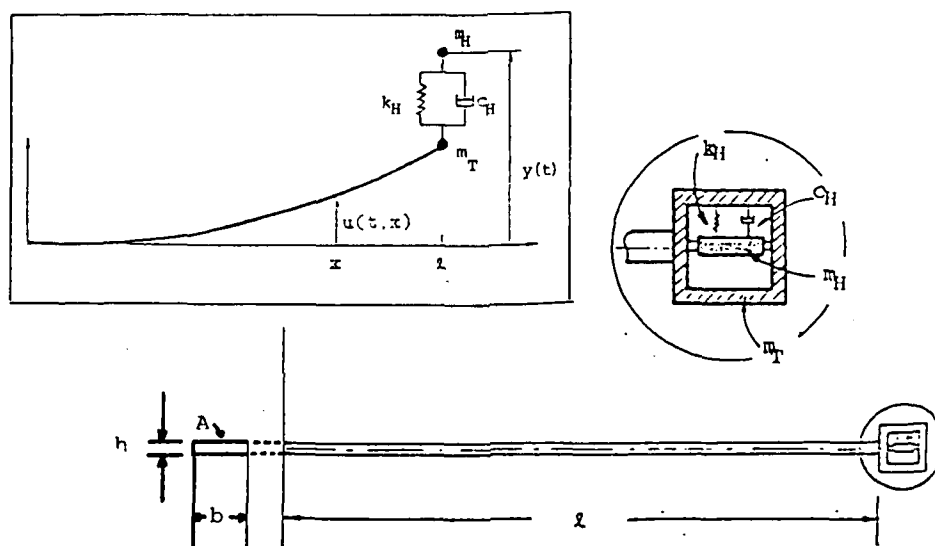


Figure 2.3

In formulating a mathematical model for the structure shown in Figure 2.3 above, we assume that the beam is of length l with uniform rectangular cross section of height h and width b . We let $u(t,x)$ and $y(t)$ denote respectively the transverse displacement of the beam at position x along its span and the displacement of the proof or hose mass, each at time t . Both are measured relative to the x -axis in the coordinate frame determined by the longitudinal axis of the beam in

its undeformed state with origin located at the beam's root or fixed end. Assuming the beam undergoes only small deformations (i.e.

$|u(t, x)| \ll l$ and $|\frac{\partial u}{\partial x}(t, x)| \ll 1$) and has a small height to span length ratio, the Euler-Bernoulli theory (see [5]) including Voigt-Kelvin viscoelastic structural damping (see [10]) yields the partial differential equation

$$(2.1) \quad \rho \frac{\partial^2 u}{\partial t^2}(t, x) + c_D I \frac{\partial^4}{\partial x^4} \frac{\partial u}{\partial t}(t, x) + EI \frac{\partial^4 u}{\partial x^4}(t, x) = 0, \\ 0 < x < l, \quad t > 0$$

where ρ is the linear mass density of the beam, E is the modulus of elasticity, c_D is the coefficient of viscosity and I is the second moment or moment of inertia of the cross sectional area A about the neutral axis. For the beam we consider here with constant rectangular cross section, $I = bh^3/12$. Since the beam is assumed to be uniform, the parameters ρ , E and c_D are taken to be constant in time and space.

Balancing forces at the free end, elementary Newtonian mechanics yields the equations of motion

$$(2.2) \quad m_T \frac{\partial^2 u}{\partial t^2}(t, l) - c_D I \frac{\partial^3}{\partial x^3} \frac{\partial u}{\partial t}(t, l) - EI \frac{\partial^3 u}{\partial x^3}(t, l) \\ = c_H \left(\frac{dy}{dt}(t) - \frac{\partial u}{\partial t}(t, l) \right) + k_H (y(t) - u(t, l)) + f(t), \quad t > 0$$

and

$$(2.3) \quad m_H \frac{d^2 y}{dt^2}(t) + c_H \left(\frac{dy}{dt}(t) - \frac{\partial u}{\partial t}(t, l) \right) + k_H (y(t) - u(t, l)) = 0, \\ t > 0$$

for the tip and hose masses m_T and m_H respectively. Here k_H is the hose stiffness, c_H is the hose damping coefficient and $f(t)$ is the externally applied force at time t due to the firing of the thrusters mounted at the tip.

Making the assumption that the rotatory inertia of the proof mass system is negligible, rotational equilibrium at the tip can be expressed as

$$(2.4) \quad c_D I \frac{\partial^2}{\partial x^2} \frac{\partial u}{\partial t}(t, \ell) + EI \frac{\partial^2 u}{\partial x^2}(t, \ell) = 0, \quad t > 0.$$

The zero displacement and zero slope constraints at the fixed end are given by

$$(2.5) \quad u(t, 0) = 0 \quad \text{and} \quad \frac{\partial u}{\partial x}(t, 0) = 0, \quad t > 0$$

respectively. Taking the structure to be initially at rest we have the initial conditions

$$(2.6) \quad u(0, x) = 0 \quad \text{and} \quad \frac{\partial u}{\partial t}(0, x) = 0, \quad 0 \leq x \leq \ell$$

and

$$(2.7) \quad y(0) = 0 \quad \text{and} \quad \frac{dy}{dt}(0) = 0.$$

In the mathematical model given by (2.1) - (2.7) above the parameters ρ , m_T and I can be measured or computed directly. The modulus of elasticity E is typically determined in the laboratory. For the most commonly used materials (including aluminum which is the material from

which the structure of interest to us here is made) its value can be readily looked up in standard engineering tables. The parameters c_D , m_H , c_H and k_H on the other hand, must be determined experimentally; that is, they will have to be identified based upon the observed response of the structure to a given input disturbance. This is one class of inverse problems which we formulate and consider below. In the system of equations (2.1) - (2.7) we explicitly modeled (albeit, in a rather simple fashion) the dynamical effects of the hose. The unknown hose parameters are then determined as the solution to an inverse problem.

An alternative approach to obtaining a model which exhibits a reasonable degree of fidelity involves a technique which is sometimes referred to as model adjustment. Starting with a simple model, the parameters are then "adjusted" so as to compensate for unmodeled dynamics. The choice of parameters to be adjusted and the resulting variations may or may not be motivated by physical considerations.

In our problem for example, we might consider a simple cantilevered beam with tip mass (i.e. $m_H = c_H = k_H = 0$) and then adjust the theoretical or measured values of E and m_T to compensate for the dynamical effects which result from the hose mass and motion. A value for the parameter c_D could also be identified if damping effects are considered significant. Model adjustment was used in [6] to obtain a model for the RPL structure upon which control design could be based.

We define an inverse problem which encompasses both of the general approaches which have been outlined above. We assume that an input disturbance described by the function $f(t)$, $t \in [0, T]$ is applied to the structure via the tip thrusters and that the linear accelera-

tion at the free end of the beam, $z(t)$, is measured and recorded for each $t \in [t_0, t_1]$ where $0 \leq t_0 \leq t_1 \leq T$. (Of course, in actual practice, z could in fact only be sampled discretely). Let R_+ denote the positive real numbers and let Q be a closed and bounded subset of R_+^6 . We seek a $\bar{q} \in Q$ which minimizes

$$J(q) = \int_{t_0}^{t_1} \left| \frac{\partial^2 u}{\partial t^2}(t, l; q) - z(t) \right|^2 dt$$

where $u(\cdot, \cdot; q)$ denotes the solution to the initial-boundary value problem (2.1) - (2.7) corresponding to $q = (m_T, E, c_D, m_H, c_H, k_H) \in Q$.

Our primary concerns in the next section will include well-posedness of the system (2.1) - (2.7), existence of a minimizer for J , and development of approximation techniques to find this minimizer.

3. Approximation Theory

A computational method for the solution of the estimation problem posed above will invariably involve finite dimensional approximation of the initial-boundary value problem (2.1) - (2.7). We have been successful in solving inverse problems for distributed parameter models for flexible structures (see, for example, [1], [2], [3], [4], [12]) using spline-based Ritz-Galerkin techniques. We apply those ideas here and derive finite element approximations based upon an abstract Hilbert space formulation of the hybrid system of ordinary and partial differential equations and boundary conditions given in (2.1) - (2.7). This abstract formulation is also useful in establishing existence, uniqueness and necessary regularity results for solutions. We briefly outline the essential features of our general approach (including theoretical convergence results) in the context of the particular problem of interest to us here.

Let $H = R^2 \times L_2(0, l)$ be endowed with the usual product space inner product

$$\langle (\zeta, \eta, \phi), (\lambda, \mu, \psi) \rangle_H = \zeta\lambda + \eta\mu + \langle \phi, \psi \rangle_0$$

and let

$$V = \{(\zeta, \eta, \phi) \in H: \phi \in H^2(0, l), \phi(0) = D\phi(0) = 0, \eta = \phi(l)\}$$

be endowed with the inner product

$$\langle (\zeta, \phi(l), \phi), (\lambda, \psi(l), \psi) \rangle_V = (\zeta - \phi(l))(\lambda - \psi(l)) + \langle D^2\phi, D^2\psi \rangle_0$$

where the symbol D is used here and below to denote the spatial differentiation operator $\frac{d}{dx}$. The space V together with the inner product $\langle \cdot, \cdot \rangle_V$ form a Hilbert space which is densely and compactly embedded in H .

We rewrite the system (2.1) - (2.7) as the abstract second order initial value problem in H

$$(3.1) \quad \hat{M}u_{tt}(t) + \hat{C}u_t(t) + \hat{K}u(t) = F(t), \quad t > 0$$

$$(3.2) \quad \delta(\hat{u}(t) + \epsilon u_t(t)) = 0, \quad t > 0$$

$$(3.3) \quad \hat{u}(0) = 0 \quad u_t(0) = 0$$

in the states $\hat{u}(t) = (y(t), u(t, l), u(t, \cdot))$. The operators $M \in L(H)$, $C: D \subset H \rightarrow H$ and $K: D \subset H \rightarrow H$ are given by

$$(3.4) \quad M(\zeta, \eta, \phi) = (m_H \zeta, m_T \eta, \rho \phi),$$

$$C(\zeta, \eta, \phi) = (c_H(\zeta - \eta), c_H(\eta - \zeta) - c_D I D^* \phi(l), c_D I D^* \phi),$$

and

$$K(\zeta, \eta, \phi) = (k_H(\zeta - \eta), k_H(\eta - \zeta) - EI D^* \phi(l), EI D^* \phi)$$

where $D = \{(\zeta, \eta, \phi) \in V: \phi \in H^1(0, l)\}$. For each $t > 0$, $F(t) = (0, f(t), 0) \in H$, $\delta: D \subset H \rightarrow R$ is given by $\delta((\zeta, \eta, \phi)) = D^* \phi(l)$ and $\epsilon = c_D/E$.

The restrictions \tilde{C} and \tilde{K} of the operators C and K that appear in equation (3.1) above to $N(\delta)$, the null space of the operator δ , have

natural extensions to bounded operators from V (which is the V -closure of $N(\delta)$) into V' , the dual of V . The extensions are defined in terms of the bilinear forms $c(\cdot, \cdot): V \times V \rightarrow R$ and $k(\cdot, \cdot): V \times V \rightarrow R$ given by

$$(3.5) \quad (\tilde{C}\hat{\phi})(\hat{\psi}) = c(\hat{\phi}, \hat{\psi}) = c_H(\zeta - \phi(l))(\lambda - \psi(l)) + c_D I \langle D^2 \phi, D^2 \psi \rangle_0$$

and

$$(3.6) \quad (\tilde{K}\hat{\phi})(\hat{\psi}) = k(\hat{\phi}, \hat{\psi}) = k_H(\zeta - \phi(l))(\lambda - \psi(l)) + EI \langle D^2 \phi, D^2 \psi \rangle_0$$

for $\hat{\phi} = (\zeta, \phi(l), \phi) \in V$ and $\hat{\psi} = (\lambda, \psi(l), \psi) \in V$.

The finite element method we develop below could be derived from standard energy considerations. While this is not the approach we take, it is worth noting that the usual energy expressions can be given in terms of the forms, operators and inner products defined above. The kinetic energy is given by

$$T_0 = \frac{1}{2} \langle M \hat{u}_t(t), \hat{u}_t(t) \rangle_H,$$

the potential or strain energy by

$$U_0 = \frac{1}{2} k(\hat{u}(t), \hat{u}(t))$$

and the Rayleigh dissipation function by

$$F_0 = \frac{1}{2} c(\hat{u}_t(t), \hat{u}_t(t)).$$

Written in its weak, variational or distributional form

$$(3.7) \quad \langle M \hat{u}_{tt}(t), \hat{\phi} \rangle_H + c(\hat{u}_t(t), \hat{\phi}) + k(\hat{u}(t), \hat{\phi}) = \langle F(t), \hat{\phi} \rangle_H,$$

$t > 0, \quad \hat{\phi} \in V$

$$(3.8) \quad \hat{u}(0) = 0 \qquad \hat{u}_t(0) = 0$$

the initial value problem (3.1) - (3.2) in H becomes an initial value problem in V' . If we assume that $f \in L_1(0,T)$ and rewrite (3.7), (3.8) as an equivalent first order vector system, the theory of abstract parabolic systems (see [9], [14]) yields the existence of a unique mapping

$$\hat{u} \in C([0,T];V) \cap H^1((0,T);V) \cap C^1([0,T];H) \cap H^2((0,T);V')$$

which satisfies (3.7), (3.8). If we are willing to assume further that f is Hölder continuous then there exists a

$$(3.9) \quad \hat{u} \in C([0,T];V) \cap C^1((0,T];V) \cap C^1([0,T];H) \cap C^2((0,T];H)$$

with $\hat{u}(t) + \epsilon \hat{u}_t(t) \in D$, $t > 0$ which uniquely satisfies the initial value problem (3.1) - (3.3).

In order to demonstrate the convergence of the approximation schemes we develop below, we shall require a somewhat more regular solution to the initial value problem (3.7), (3.8) than either of the conditions on f stated above can guarantee. In addition to (3.9), we shall require that $\hat{u} \in H^2((0,T);V)$. This can be guaranteed (see [7]) if we assume that $f \in H^1(-\tau,T)$ for some $\tau > 0$ with $f(t) = 0$, $t < 0$ and we modify our original mathematical model so that

$$(3.10) \quad F(t) = f(t)\hat{\theta}, \qquad t \in [-\tau,T]$$

for some $\hat{\theta} = (0, \theta(1), \theta)$, a fixed element in V . We note that with $\hat{\theta}$

chosen appropriately in V , F given by (3.10) may in fact represent an improved model of reality when compared with our present choice of F where $\hat{\theta} = (0, 1, 0) \in H$.

Central to our approach is a cubic spline based Galerkin approximation to the initial value problem (3.7), (3.8). For each $N = 1, 2, \dots$

let Δ^N denote the uniform mesh $\{0, \frac{\ell}{N}, \frac{2\ell}{N}, \dots, \ell\}$ on $[0, \ell]$ and let

$\{B_j^N\}_{j=-1}^{N+1}$ denote the usual cubic B-splines defined with respect to the nodal set Δ^N (see [11], [13]). Briefly, each B_j^N is a C^2 function on

$[0, \ell]$ which is a cubic polynomial on each subinterval $[(k-1)\frac{\ell}{N}, k\frac{\ell}{N}]$,

$k = 1, 2, \dots, N$. The support of B_j^N is $[(j-2)\frac{\ell}{N}, (j+2)\frac{\ell}{N}] \cap [0, \ell]$ with

$B_j^N(\frac{\ell}{N}) = 4$, $DB_j^N(\frac{\ell}{N}) = 0$, $B_j^N((j+1)\frac{\ell}{N}) = 1$, and $DB_j^N((j+1)\frac{\ell}{N}) = \mp \frac{N}{\ell}$.

Defining $\{\beta_j^N\}_{j=1}^{N+1}$ by $\beta_1^N = B_0^N - 2B_1^N - 2B_{-1}^N$ and $\beta_j^N = B_j^N$, $j=2, 3, \dots, N+1$,

we have $\beta_j^N(0) = D\beta_j^N(0) = 0$, $j = 1, 2, \dots, N+1$. With $\hat{\beta}_0 = (1, 0, 0)$ and

$\hat{\beta}_j^N = (0, \beta_j^N(\ell), \beta_j^N)$, $j = 1, 2, \dots, N+1$, $V^N = \text{span } \{\beta_j^N\}_{j=0}^{N+1}$ is an $N+2$

dimensional subspace of V .

The Galerkin equations in V^N corresponding to (3.7), (3.8) for $\hat{u}^N(t) \in V^N$ are given by

$$(3.11) \quad \langle \hat{M} \hat{u}_{tt}^N(t), \hat{\beta}_j^N \rangle_H + c(\hat{u}_t^N(t), \hat{\beta}_j^N) + k(\hat{u}^N(t), \hat{\beta}_j^N) = \langle F(t), \hat{\beta}_j^N \rangle_H, \\ t > 0, \quad j = 0, 1, 2, \dots, N+1$$

$$(3.12) \quad \hat{u}^N(0) = 0 \qquad \hat{u}_t^N(0) = 0.$$

Setting

$$\hat{u}^N(t) = \sum_{j=0}^{N+1} w_j^N(t) \hat{\beta}_j^N, \quad t \geq 0,$$

the initial value problem (3.11), (3.12) in V^N is equivalent to the linear, nonhomogeneous, second order $N+2$ - vector system

$$(3.13) \quad M^N \frac{d^2 w^N}{dt^2}(t) + C^N \frac{dw^N}{dt}(t) + K^N w^N(t) = F^N(t), \quad t > 0$$

$$(3.14) \quad w^N(0) = 0 \quad \frac{dw^N}{dt}(0) = 0$$

where $w^N(t) = (w_0^N(t), w_1^N(t), \dots, w_{N+1}^N(t))^T$. The entries in the $(N+2) \times (N+2)$ matrices M^N , C^N and K^N are given by

$$M_{1,j}^N = \langle M \hat{\beta}_1^N, \hat{\beta}_j^N \rangle_H,$$

$$C_{1,j}^N = c(\hat{\beta}_1^N, \hat{\beta}_j^N),$$

and

$$K_{1,j}^N = k(\hat{\beta}_1^N, \hat{\beta}_j^N),$$

$1, j = 0, 1, 2, \dots, N+1$ respectively. For each $t > 0$ the components in the $N+2$ - vector $F^N(t)$ are given by $F_1^N(t) = \langle F(t), \hat{\beta}_1^N \rangle_H = f(t) \beta_1^N(l)$ or, recalling (3.10), by

$$F_1^N(t) = f(t) \langle \hat{\theta}, \hat{\beta}_1^N \rangle_H = f(t) (\theta(l) \beta_1^N(l) + \langle \theta, \beta_1^N \rangle_0),$$

$$i = 0, 1, 2, \dots, N+1.$$

We consider the sequence of approximating finite dimensional identification problems which consist of finding $\bar{q}^N \in Q$ which minimizes

$$(3.15) \quad J^N(q) = \int_{t_0}^{t_1} \left| \frac{\partial^2 u^N}{\partial t^2}(t, l; q) - z(t) \right|^2 dt$$

where for each $q \in Q$, $\hat{u}^N(t; q) = (y^N(t; q), u^N(t, l; q), u^N(t, \cdot; q))$ is the unique solution to the initial value problem (3.11), (3.12) in V^N corresponding to $q = (m_T, E, c_D, m_H, c_H, k_H) \in Q$. In actual practice, for a given $q \in Q$, $J^N(q)$ is computed as

$$J^N(q) = \int_{t_0}^{t_1} \left| w_{N-1}^N(t; q) + 4w_N^N(t; q) + w_{N+1}^N(t; q) - z(t) \right|^2 dt$$

where $w^N(\cdot; q) = (w_0^N(\cdot; q), \dots, w_{N+1}^N(\cdot; q))^T$ is the unique solution to the $N+2$ - vector system (3.13), (3.14) corresponding to $q \in Q$.

With finite dimensional state constraints, the solution of the N^{th} estimation problem above is, at least in principle, routine. For inverse problems which are closely related to the one we treat here, our earlier numerical studies have shown that satisfactory results can be obtained using any one of a number of standard computational techniques for least squares minimization (for example, Newton's method, conjugate gradient, steepest descent, Levenberg-Marquardt, etc., see [2]).

Our fundamental theoretical result is that each of the approximating identification problems and the original problem have solutions. Moreover, we show that the solutions to the approximating problems, in some sense, approximate solutions to the original problem. We require the following lemma.

Lemma 3.1 Suppose $\{q^N\} \subset Q$ with $q^N \rightarrow q^0$ as $N \rightarrow \infty$. Let $\hat{u}^N(\cdot; q^N)$ denote the unique solution to the initial value problem (3.11), (3.12) corresponding to q^N and let $\hat{u}(\cdot; q^0)$ denote the unique solution to the initial value problem (3.7), (3.8) corresponding to q^0 . If $u(\cdot; q^0) \in H^2((0, T); V)$ then

$$(3.16) \quad \int_0^T \left| \hat{u}_{tt}^N(t; q^N) - \hat{u}_{tt}(t; q^0) \right|_H^2 dt \rightarrow 0$$

as $N \rightarrow \infty$.

Proof

For each $N = 1, 2, \dots$ let P^N denote the orthogonal projection of H onto V^N defined with respect to the standard inner product on H , $\langle \cdot, \cdot \rangle_H$. Using the approximation theoretic properties of interpolatory splines, it is not difficult to show that (see [3])

$$(3.17) \quad \lim_{N \rightarrow \infty} \left| (P^N - I)(\zeta, \eta, \phi) \right|_H = 0$$

for each $(\zeta, \eta, \phi) \in H$ and that

$$(3.18) \quad \lim_{N \rightarrow \infty} \left| (P^N - I)\hat{\phi} \right|_V = 0$$

for each $\hat{\phi} \in V$.

For $q = (m_T, E, c_D, m_H, c_H, k_H) \in Q$ it is immediately clear that M , $c(\cdot, \cdot)$ and $k(\cdot, \cdot)$, the operator and forms defined in (3.4), (3.5) and (3.6) respectively depend upon q . For $q^0 = (m_T^0, E^0, c_D^0, m_H^0, c_H^0, k_H^0) \in Q$ and $q^N = (m_T^N, E^N, c_D^N, m_H^N, c_H^N, k_H^N) \in Q$ we adopt the shorthand notation $M^0 = M(q^0)$, $c^0(\cdot, \cdot) = c(q^0)(\cdot, \cdot)$, $k^0(\cdot, \cdot) = k(q^0)(\cdot, \cdot)$, $M^N = M(q^N)$, $c^N(\cdot, \cdot) = c(q^N)(\cdot, \cdot)$ and $k^N(\cdot, \cdot) = k(q^N)(\cdot, \cdot)$. Similarly, we denote $\hat{u}(\cdot; q^0)$ and $\hat{u}^N(\cdot; q^N)$ by \hat{u}^0 and \hat{u}^N respectively.

From (3.17), the assumption that $\hat{u}^0 \in H^2((0, T); V)$ and the inequality

$$\begin{aligned} & \int_0^T \left| \hat{u}_{tt}^N(t) - \hat{u}_{tt}^0(t) \right|_H^2 dt \\ & \leq 2 \int_0^T \left| \hat{u}_{tt}^N(t) - P^N \hat{u}_{tt}^0(t) \right|_H^2 dt + 2 \int_0^T \left| (I - P^N) \hat{u}_{tt}^0(t) \right|_H^2 dt \end{aligned}$$

it is clear that we need only to consider the first term on the right hand side of the above estimate.

Letting $\hat{v}^N(t) = \hat{u}^N(t) - P^N \hat{u}^0(t)$ for $t \geq 0$, (3.7), (3.8), (3.11), (3.12) and $\hat{v}^N \subset V$ imply

$$\begin{aligned} (3.19) \quad & \langle M^N \hat{v}_{tt}^N, \hat{\phi}^N \rangle_H + c^N(\hat{v}_t^N, \hat{\phi}^N) + k^N(\hat{v}^N, \hat{\phi}^N) \\ & = \langle M^N (I - P^N) \hat{u}_{tt}^0, \hat{\phi}^N \rangle_H + \langle (M^0 - M^N) \hat{u}_{tt}^0, \hat{\phi}^N \rangle_H \\ & + c^N((I - P^N) \hat{u}_t^0, \hat{\phi}^N) + c^0(\hat{u}_t^0, \hat{\phi}^N) - c^N(\hat{u}_t^0, \hat{\phi}^N) \\ & + k^N((I - P^N) \hat{u}^0, \hat{\phi}^N) + k^0(\hat{u}^0, \hat{\phi}^N) - k^N(\hat{u}^0, \hat{\phi}^N), \quad t > 0, \hat{\phi}^N \in V^N \end{aligned}$$

$$(3.20) \quad \hat{v}^N(0) = 0$$

$$\hat{v}_t^N(0) = 0.$$

Choosing $\hat{\phi}^N = \hat{v}_{tt}^N(t) \in V^N$, from (3.19) we obtain

$$\begin{aligned} & \langle M^N \hat{v}_{tt}^N, \hat{v}_{tt}^N \rangle_H + c^N(\hat{v}_t^N, \hat{v}_{tt}^N) \\ &= \langle M^N(I-P^N) \hat{u}_{tt}^0, \hat{v}_{tt}^N \rangle_H + \langle (M^0 - M^N) \hat{u}_{tt}^0, \hat{v}_{tt}^N \rangle_H \\ &+ \frac{d}{dt} c^N((I-P^N) \hat{u}_t^0, \hat{v}_t^N) - c^N((I-P^N) \hat{u}_{tt}^0, \hat{v}_t^N) \\ &+ \frac{d}{dt} \{c^0(\hat{u}_t^0, \hat{v}_t^N) - c^N(\hat{u}_t^0, \hat{v}_t^N)\} - \{c^0(\hat{u}_{tt}^0, \hat{v}_t^N) - c^N(\hat{u}_{tt}^0, \hat{v}_t^N)\} \\ &+ \frac{d}{dt} k^N((I-P^N) \hat{u}_t^0, \hat{v}_t^N) - k^N((I-P^N) \hat{u}_{tt}^0, \hat{v}_t^N) \\ &+ \frac{d}{dt} \{k^0(\hat{u}_t^0, \hat{v}_t^N) - k^N(\hat{u}_t^0, \hat{v}_t^N)\} - \{k^0(\hat{u}_{tt}^0, \hat{v}_t^N) - k^N(\hat{u}_{tt}^0, \hat{v}_t^N)\} \\ &- \frac{d}{dt} k^N(\hat{v}_t^N, \hat{v}_t^N) + k^N(\hat{v}_t^N, \hat{v}_t^N), \quad t > 0. \end{aligned}$$

Integrating the above expression from 0 to t and recalling (3.20), we find

$$\begin{aligned} (3.21) \quad & \int_0^t \langle M^N \hat{v}_{ss}^N, \hat{v}_{ss}^N \rangle_H ds + \frac{1}{2} c^N(\hat{v}_t^N, \hat{v}_t^N) \\ &= \int_0^t \{ \langle M^N(I-P^N) \hat{u}_{ss}^0, \hat{v}_{ss}^N \rangle_H - \langle (M^0 - M^N) \hat{u}_{ss}^0, \hat{v}_{ss}^N \rangle_H \\ &- c^N((I-P^N) \hat{u}_{ss}^0, \hat{v}_s^N) - (c^0(\hat{u}_{ss}^0, \hat{v}_s^N) - c^N(\hat{u}_{ss}^0, \hat{v}_s^N)) \\ &- k^N((I-P^N) \hat{u}_s^0, \hat{v}_s^N) - (k^0(\hat{u}_s^0, \hat{v}_s^N) - k^N(\hat{u}_s^0, \hat{v}_s^N)) \\ &+ k^N(\hat{v}_s^N, \hat{v}_s^N) \} ds \\ &+ c^N((I-P^N) \hat{u}_t^0, \hat{v}_t^N) + (c^0(\hat{u}_t^0, \hat{v}_t^N) - c^N(\hat{u}_t^0, \hat{v}_t^N)) \end{aligned}$$

$$+ k^N((I-P^N)\hat{u}^0, \hat{v}_t^N) + (k^0(\hat{u}^0, \hat{v}_t^N) - k^N(\hat{u}^0, \hat{v}_t^N)) - k^N(\hat{v}^N, \hat{v}_t^N).$$

We recall that Q has been assumed to be a closed and bounded subset of R_+^6 and observe therefore that the forms $c^0(\cdot, \cdot)$, $c^N(\cdot, \cdot)$, $k^0(\cdot, \cdot)$ and $k^N(\cdot, \cdot)$ are uniformly bounded. These two facts together with the repeated application of the inequality

$$\langle a, b \rangle \leq |a| |b| \leq \alpha |a|^2 + \frac{1}{4\alpha} |b|^2, \quad \alpha > 0$$

in (3.21) yield the estimate

$$\begin{aligned} & \int_0^t |\hat{v}_{ss}^N|_H^2 ds + |\hat{v}_t^N|_V^2 \\ & \leq \gamma_0 \left\{ \int_0^t \left(\frac{1}{4\alpha} |(I-P^N)\hat{u}_{ss}^0|_H^2 + \alpha |\hat{v}_{ss}^N|_H^2 \right. \right. \\ & \quad + \frac{1}{4\alpha} (|\hat{m}_H^N - \hat{m}_H^0|^2 + |\hat{m}_T^N - \hat{m}_T^0|^2) |\hat{u}_{ss}^0|_H^2 + \alpha |\hat{v}_{ss}^N|_H^2 + |(I-P^N)\hat{u}_{ss}^0|_V^2 \\ & \quad + |\hat{v}_s^N|_V^2 + (|\hat{c}_H^N - \hat{c}_H^0|^2 + |\hat{c}_D^N - \hat{c}_D^0|^2) |\hat{u}_{ss}^0|_V^2 + |\hat{v}_s^N|_V^2 \\ & \quad + |(I-P^N)\hat{u}_s^0|_V^2 + |\hat{v}_s^N|_V^2 + (|\hat{k}_H^N - \hat{k}_H^0|^2 + |\hat{E}^N - \hat{E}^0|^2) |\hat{u}_s^0|_V^2 + |\hat{v}_s^N|_V^2 \\ & \quad \left. \left. + |\hat{v}_s^N|_V^2 \right) ds + \frac{1}{4\alpha} |(I-P^N)\hat{u}_t^0|_V^2 + \alpha |\hat{v}_t^N|_V^2 \right. \\ & \quad + \frac{1}{4\alpha} (|\hat{c}_H^N - \hat{c}_H^0|^2 + |\hat{c}_D^N - \hat{c}_D^0|^2) |\hat{u}_t^0|_V^2 + \alpha |\hat{v}_t^N|_V^2 + \frac{1}{4\alpha} |(I-P^N)\hat{u}^0|_V^2 \\ & \quad \left. + \alpha |\hat{v}_t^N|_V^2 + \frac{1}{4\alpha} (|\hat{k}_H^N - \hat{k}_H^0|^2 + |\hat{E}^N - \hat{E}^0|^2) |\hat{u}^0|_V^2 + \alpha |\hat{v}_t^N|_V^2 \right\} \end{aligned}$$

$$+ \frac{1}{4\alpha} |\hat{v}^N|_V^2 + \alpha |\hat{v}_t^N|_V^2)$$

where γ_0 is a positive constant. Choosing $\alpha > 0$ sufficiently small, we find

$$(3.22) \quad \int_0^t |\hat{v}_{ss}^N(s)|_H^2 ds + |\hat{v}_t^N(t)|_V^2 \leq \sigma_0(t) + \int_0^t \sigma_1(s) ds + \gamma_1 \int_0^t |\hat{v}_s^N(s)|_V^2 ds$$

where

$$\begin{aligned} \sigma_0(t) &= \gamma_2 \{ |(I-P^N)\hat{u}^0(t)|_V^2 + |(I-P^N)\hat{u}_t^0(t)|_V^2 \\ &\quad + |q^N - q^0|^2 (|\hat{u}^0(t)|_V^2 + |\hat{u}_t^0(t)|_V^2) + |\hat{v}^N(t)|_V^2 \} \\ \sigma_1(t) &= \gamma_3 \{ |(I-P^N)\hat{u}_t^0(t)|_V^2 + |(I-P^N)\hat{u}_{tt}^0(t)|_V^2 \\ &\quad + |q^N - q^0|^2 (|\hat{u}_t^0(t)|_V^2 + |\hat{u}_{tt}^0(t)|_V^2) \} \end{aligned}$$

and γ_i , $i = 1, 2, 3$ are positive constants which do not depend on N .

Choosing $\hat{\phi}^N = \hat{v}_t^N(t) \in V^N$ in (3.19), arguments similar to those used above (see [2], [3]) yield

$$(3.23) \quad \lim_{N \rightarrow \infty} |\hat{v}^N(t)|_V^2 = 0$$

for each $t \in [0, T]$. Using $\hat{u}^0 \in H^1((0, T); V)$, (3.18) and an application of the Gronwall inequality to (3.22) we obtain the desired result.

We note that we also obtain

$$(3.24) \quad \lim_{N \rightarrow \infty} \left| \hat{v}_t^N(t) \right|_V^2 = 0$$

for each $t \in [0, T]$. From (3.23) and (3.24) we find $\left| \hat{u}^N(t; q^N) - \hat{u}(t; q^0) \right|_V \rightarrow 0$ and $\left| \hat{u}_t^N(t; q^N) - \hat{u}_t(t; q^0) \right| \rightarrow 0$ as $N \rightarrow \infty$ for each $t \in [0, T]$.

We remark that it is the L_2 convergence (more precisely, H convergence) in (3.16) which necessitates, at least in theory, that we be provided with distributed time observations (i.e. observations which are continuous in time). It is clear from (3.23) and (3.24) that for fits based upon displacement, velocity or slope, time-sampled measurements are sufficient. Of course when the approximating optimization problems are solved, the integral least squares performance indices (3.15) are discretized. Consequently, in practice, only discrete measurements of linear acceleration at the tip are required.

Theorem 3.1 Each of the approximating identification problems has a solution \bar{q}^N . The sequence $\{\bar{q}^N\} \subset Q$ admits a convergent subsequence $\{\bar{q}^{N_j}\}$ with $\bar{q}^{N_j} \rightarrow \bar{q} \in Q$ as $j \rightarrow \infty$. If for each $q \in Q$, $\hat{u}(\cdot; q)$, the unique solution to the initial value problem (3.7), (3.8) corresponding to q , is an element in $H^2((0, T); V)$ then \bar{q} is a solution to the original identification problem. In addition, the limit point of any convergent subsequence of $\{\bar{q}^N\}$ is a solution to the original identification problem as well.

Proof Standard continuous dependence results for linear ordinary differential equations, the fact that Q has been assumed to be a

closed and bounded subset of R^6 and the form of J^N are sufficient to conclude that a solution $\bar{q}^N \in Q$ to the N^{th} approximating identification problem exists. Once again since Q is a closed and bounded (and therefore compact) subset of R^6 , the sequence $\{\bar{q}^N\} \subset Q$ admits a convergent subsequence. If $\{\bar{q}^{N_j}\} \subset \{\bar{q}^N\}$ with $\bar{q}^{N_j} \rightarrow \bar{q} \in Q$ as $j \rightarrow \infty$ and q is any point in Q , then two applications of Lemma 3.1 (the second one with the constant sequence $\{q\}$) yield

$$J(\bar{q}) = \lim_{j \rightarrow \infty} J^{N_j}(\bar{q}^{N_j}) \leq \lim_{j \rightarrow \infty} J^{N_j}(q) = J(q)$$

and the theorem is proved.

Although Theorem 3.1 above guarantees only subsequential convergence, in all test and simulation examples we have considered, we in fact observe the convergence of the sequence $\{\bar{q}^N\}$ itself to the optimal parameters \bar{q} . Also, it is not difficult to verify that with only minor modification (see [2]) the approximation scheme reported on here (together with the convergence theory outlined in the lemma and theorem above) could be applied to inverse problems involving the estimation of spatially varying parameters (such as linear mass density ρ , flexural stiffness EI , or damping coefficient $c_D I$) which appear in the equations (2.1) - (2.4). We note of course that when either EI or $c_D I$ are spatially varying, the Euler-Bernoulli equation and corresponding boundary conditions are of a slightly different form than those given in (2.1) - (2.4) (see [3]).

4. Numerical Results

We used our scheme to attempt to solve the inverse problem which was posed above with data obtained from an experiment on the RPL structure. We report on our findings and observations here.

All computer codes were written in Fortran and run on the IBM 3081 at the University of Southern California. The approximating finite dimensional least-squares minimization problems were solved using the IMSL implementation of the Levenberg-Marquardt algorithm (routine ZXSSQ), an iterative Newton's method-steepest descent hybrid (see[2]). The second order $N+2$ - vector systems (3.13), (3.14) were solved (integrated) in each iteration (for the evaluation of J^N and its gradient) using Gear's method for stiff systems (IMSL routine DGEAR). The integral least squares performance index was approximated by a discrete sum over a uniform mesh on $[t_0, t_1]$. The integral inner products in the definitions of the matrices M^N , C^N and K^N were computed using a composite two point Gauss-Legendre quadrature rule.

The second time derivative of w^N , or generalized acceleration, $\frac{d^2 w^N}{dt^2}$, was computed using a second order centered difference on the generalized displacement,

$$(4.1) \quad \frac{d^2 w^N}{dt^2}(t) = \frac{w^N(t+\Delta) - 2w^N(t) + w^N(t-\Delta)}{\Delta^2}.$$

We found this to be a somewhat more stable method for computing acceleration (an unbounded measurement) than was a first order centered difference on the generalized velocity,

$$(4.2) \quad \frac{d^2 w^N}{dt^2}(t) = \frac{\frac{dw^N}{dt}(t + \frac{\Delta}{2}) - \frac{dw^N}{dt}(t - \frac{\Delta}{2})}{\Delta}.$$

Either of the time differencing formulas (4.1) or (4.2) proved to be significantly more stable than using the differential equation (3.13)

directly to compute $\frac{d^2 w^N}{dt^2}(t)$ via an inversion of M^N . As to why this was so, we can only offer the conjecture that the time differencing provided, at least to a certain extent, some filtration of the signal.

Before turning our attention to the experimental data, we tested our scheme with simulated data. "True" values for the unknown parameters c_D (actually $c_D I$), m_H , c_H and k_H were chosen and a quintic spline-based semi-discrete Galerkin scheme applied to the initial value problem (3.7), (3.8) was used to generate data.

Setting $\rho = .03$, $m_T = .15$, $EI = 80.0$, $l = 4.0$ and

$$f(t) = \begin{cases} 1.0 & 0 \leq t \leq 0.05 \\ 0.0 & 0.05 < t \leq 5.0, \end{cases}$$

the fit was carried out based upon observations of linear acceleration at the tip at times $t_1 = .11$, $i = 2, 3, \dots, 50$. We note that this is equivalent to taking $t_0 = .1$, $t_1 = 5.0$ and using a standard rectangle rule with uniform mesh spacing .1 to discretize the integral appearing in the definition of the least squares performance index J^N . The initial estimates $c_D I = .0035$, $m_H = .035$, and $k_H = .4$ were used to start the iterative optimization procedure. In (4.1), Δ was taken to be .1. Our results are summarized in Table 4.1 below.

N	\bar{C}_{DI}^N	\bar{m}_H^N	\bar{C}_H^N	\bar{k}_H^N	$J^N(\bar{q}^N)$
2	.037537	.039471	.003428	.298626	2.57×10^{-1}
3	.066997	.039485	.003907	.298875	4.37×10^{-2}
4	.005063	.039777	.003997	.299455	5.06×10^{-3}
5	.005667	.039899	.003971	.299787	7.66×10^{-4}
6	.005049	.040035	.004006	.300087	4.63×10^{-5}
True value	.005000	.040000	.004000	.300000	
Initial Estimate	.003500	.035000	.003500	.400000	

Table 4.1

The experiment which we describe below was carried out for us on the RPL structure by Dr. Michel A. Floyd, formerly of the Control and Flight Dynamics Division of the Charles Stark Draper Laboratory and the Department of Aeronautics and Astronautics, MIT.

The air bearing table was clamped so that the central hub could not rotate. The thruster lines for one of the active appendages was set to 300 psi and the thruster was fired for .05 seconds (50 milliseconds). With the appendage initially at rest, the firing of the thruster was assumed to have begun at time $t = 0$. Linear acceleration at the tip was observed over the time interval 0 to 5 seconds. With a sampling period of .005 seconds (5 milliseconds) a total of 1000 measurements were recorded. The data is plotted in Figure 4.1 below. The scale factor for the accelerometer is 5 volts/g ($g = 32 \text{ ft/sec}^2$).

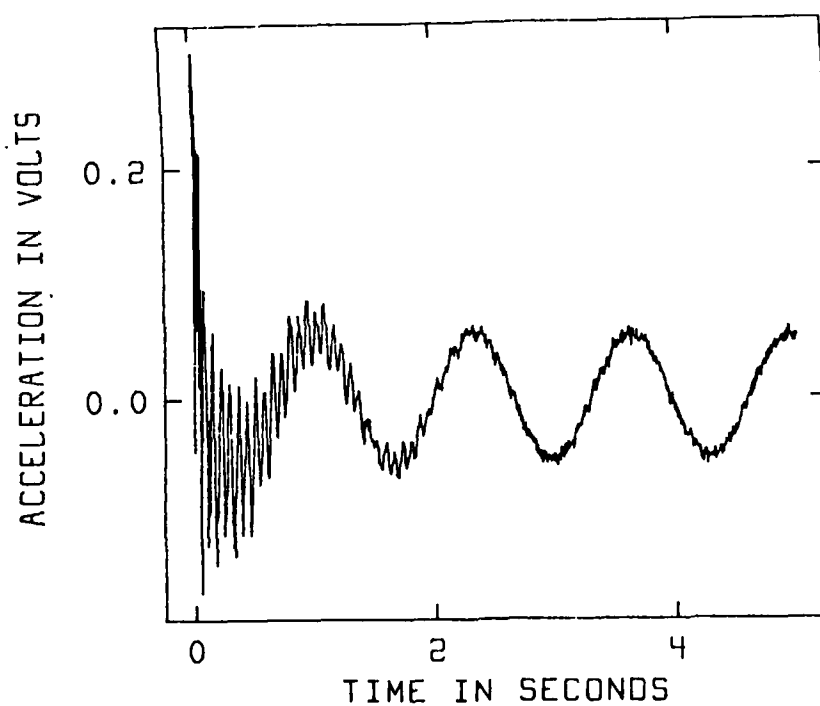


Figure 4.1

The noticeably higher frequency (≈ 14 Hz) component of the data is a torsional mode of the arm excited by the motion of the thruster valve mechanisms and inertial and elastic forces applied to the tip of the arm by the nitrogen supply hose. The opening or closing of the solenoidal valve in the thruster generates an inertial force which acts as a torque on the tip of the arm. Consequently, torsional modes are excited. Also, in addition to modifying transverse bending characteristics, since the hose is attached to the top of the arm, its horizontal motion will tend to generate torques which have a "twisting" effect. Although the accelerometer is mounted at the

center of the arm (and therefore on a nodal line of the longitudinal torsional modes, if we assume vertical symmetry), as the arm twists, the accelerometer picks up a component of the earth's gravitational force. Since the first torsional mode has a much higher frequency than either of the first two flexible modes (.75 Hz and 7.5 Hz, as identified from an FFT of the data) and since it is rapidly damped, we neglected its contribution to the accelerometer signal, treating it as white noise, and left it unmodeled. A detailed discussion of the causes of the excitation of the torsional modes and its effect on the transverse bending characteristics of the active appendages can be found in [6].

The physical characteristics of the structure are as follows. The arm is made of aluminum and is 4 feet in length, 6 inches in width and .125 inches in height. From this we obtain $l = 4.0$ ft, $\rho = .027$ slug/ft and $I = 4.71 \times 10^{-8}$ (ft)⁴. The theoretically predicted value for E is 15.84×10^8 lb/(ft)². The mass of the thruster assembly was determined to be $m_T = .149$ slug. From the calibration table in [6], we find that a hose pressure of 300 psi is equivalent to a force of .297 lb. We set therefore

$$f(t) = \begin{cases} 0.297 \text{ lb} & 0 \leq t \leq 0.05 \\ 0.0 & 0.05 < t \leq 5.0 \end{cases}$$

To serve as a basis for comparison, we neglected the hose effects and structural damping (i.e. we chose $c_D = m_H = c_H = k_H = 0$) and used the standard Euler-Bernoulli model with the parameters ρ , E , I and m_T and input f as specified above to generate the plot of linear acceleration at the tip given in Figure 4.2.

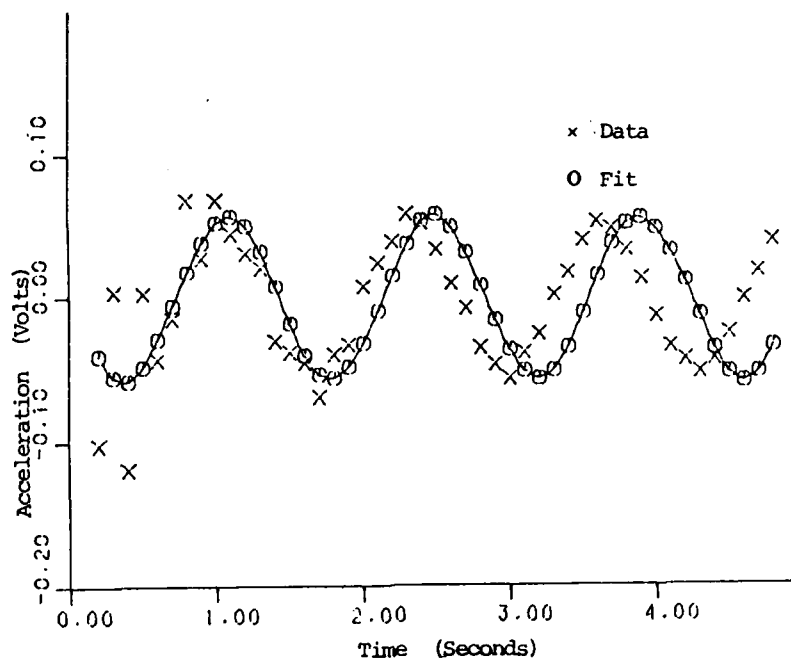


Figure 4.2

The plot was obtained by integrating the initial value problem (3.13), (3.14) with $N = 4$ and then using (4.1) to compute the acceleration at the free end. The residuals $(\frac{\partial^2 u}{\partial t^2}(t, \ell) - \frac{\partial^2 u^N}{\partial t^2}(t, \ell))$ over the time interval $[0, 5]$ are plotted in Figure 4.3. The sum of the squares of the residuals (at intervals of .1 seconds) was found to be 3.03.

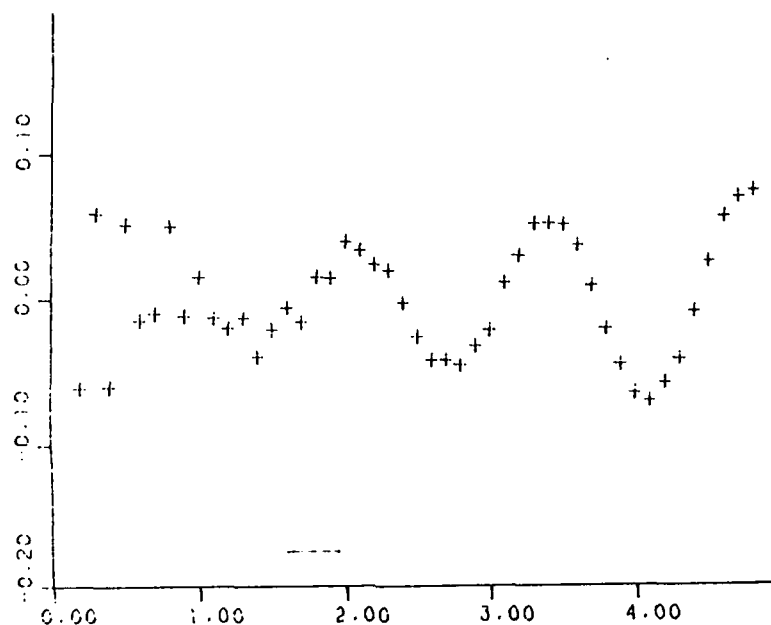


Figure 4.3

Using the data on the interval 3.0 to 5.0 (where the contribution from the torsional modes has been significantly damped) with a sampling period of .1 seconds we used our scheme with $N = 4$ to obtain optimal estimates for the coefficient of viscosity c_D and the hose parameters m_H , c_H and k_H . In the set of runs we are about to describe the values of E and m_T were held fixed at their theoretically predicted values. A rough calculation based upon "matching" the first two observed natural frequencies of the data with the first two modal frequencies of the model was used to obtain a crude initial estimate

for the ratio k_H/m_H . Then, using our scheme to minimize over the parameters m_H and k_H only, we obtained the optimal values shown in Table 4.2 below. Integrating the system (3.13), (3.14) over the time interval $[0,5]$ with m_H and k_H set to the values in the table and $c_D = c_H = 0$ the sum of the squares of the residuals (at intervals of .1 seconds) was found to be .73.

$m_H(\text{slug})$	$k_H(\text{lb/ft})$
.039269	.339935

Table 4.2

Next, holding m_H and k_H fixed at the values shown in Table 4.2, a search on c_H was carried out (the initial estimate for c_H was taken to be zero and c_D was held fixed at zero). Then using the resulting values of m_H , c_H and k_H as initial estimates, a fit over all three parameters was performed. The result is shown in Table 4.3. The sum of the squares of the residuals was found to be .728.

$m_H(\text{slug})$	$c_H(\text{lb}\cdot\text{sec/ft})$	$k_H(\text{lb/ft})$
.043431	.004056	.351385

Table 4.3

Continuing to use the same procedure to generate "start up" values, we

eventually used our scheme to search over all four parameters c_D , m_H , c_H and k_H simultaneously obtaining the values given in Table 4.4 and the fit plotted in Figure 4.4. The residuals are plotted in Figure 4.5. The sum of their squares was computed to be .70.

$c_D(\text{lb}\cdot\text{sec}/(\text{ft})^2)$	$m_H(\text{slug})$	$c_H(\text{lb}\cdot\text{sec}/\text{ft})$	$k_H(\text{lb}/\text{ft})$
127.40	.0801	.007804	.412977

Table 4.4

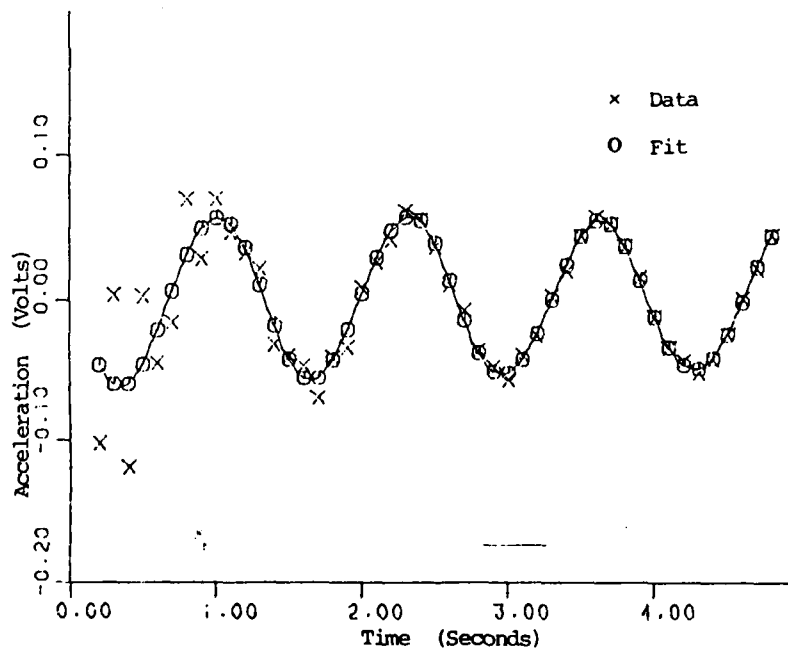


Figure 4.4

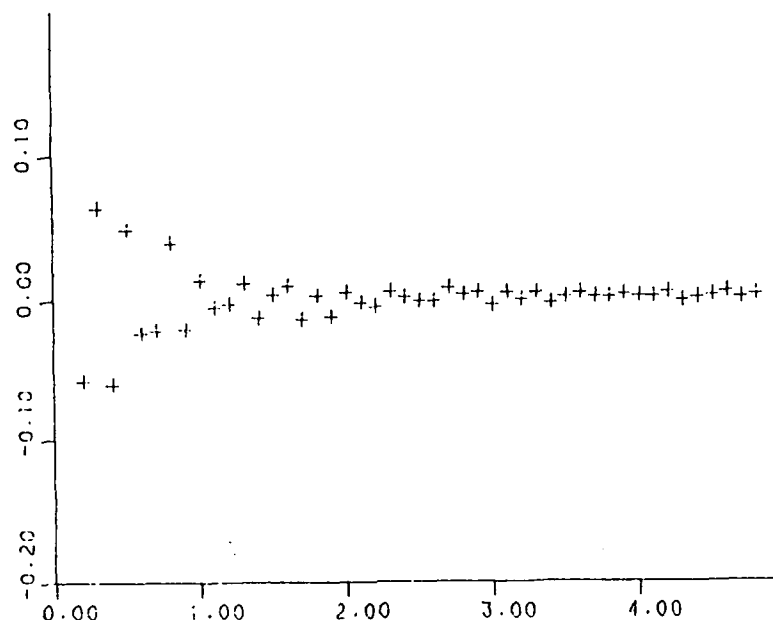


Figure 4.5

In designing a controller for the RPL experiment, Floyd in [6] used model adjustment to tune a simple, undamped, cantilevered beam with tip mass model for the active arms (i.e. the arms with the hoses) of the structure. He used the following procedure. The air bearing table was locked in a stationary position. With the hose depressurized, an impulsive force was applied to the beam and linear acceleration at the tip was measured and recorded. Based upon the physical assumption that with the hose depressurized, the presence of the hose serves only to add mass to the tip of the arm, the parameter m_T was

adjusted so that the first mode or frequency of the model agreed with the first observed cantilever mode (obtained via an FFT) of the data. Then, with the hose pressurized, the same experimental procedure was carried out. This time however, the modulus of elasticity E of the beam was adjusted to compensate for the variation in stiffness which results from the presence of the hose. The adjusted values of the tip mass, \bar{m}_T , and modulus of elasticity, \bar{E} , obtained by Floyd are given in Table 4.5 below.

\bar{m}_T (slug)	\bar{E} (lb/(ft) ²)
.254	17.31×10^8

Table 4.5

We integrated the system (3.13), (3.14) using the adjusted values of m_T and E given in the table (and $c_D = m_H = c_H = k_H = 0$) and obtained the plot shown in Figure 4.6. The corresponding residuals are plotted in Figure 4.7. The sum of the squares of the residuals was computed to be 5.1.

Starting with the same basic model, we used our scheme to determine the values of m_T and E which minimize the sum of the squares of the residuals over the time interval [3.0, 5.0] with a sampling period of .1 seconds. Taking the theoretically predicted values of m_T and E ($m_T = .149$ slug, $E = 15.84 \times 10^8$ lb/(ft)²) as start up values for the optimization routine yielded the results given in Table 4.6.

The corresponding fit and residuals are plotted in Figures 4.8 and 4.9 respectively below. The sum of the squares of the residuals (over the interval $[0,5]$) was computed to be .73.

m_T (slug)	E (lb/(ft) ²)
.185	21.95×10^8

Table 4.6

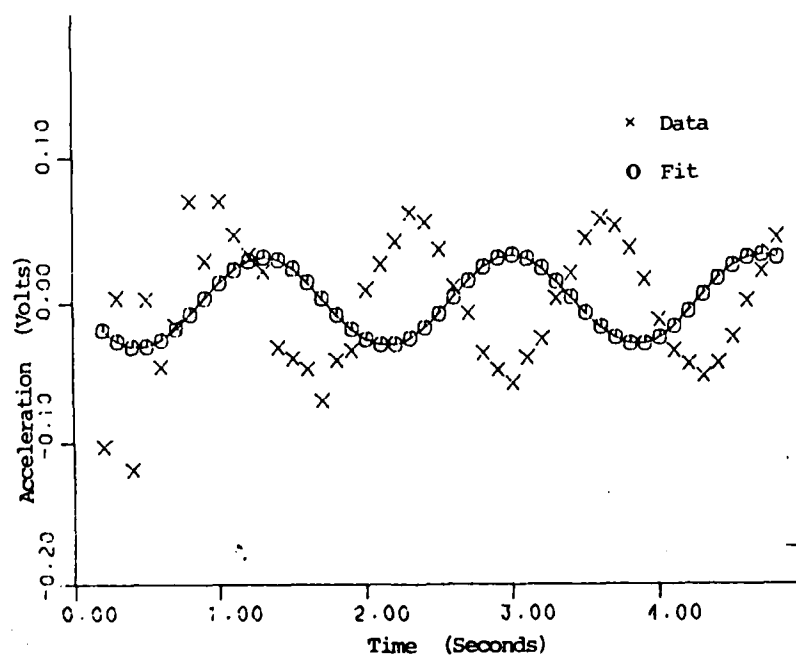


Figure 4.6

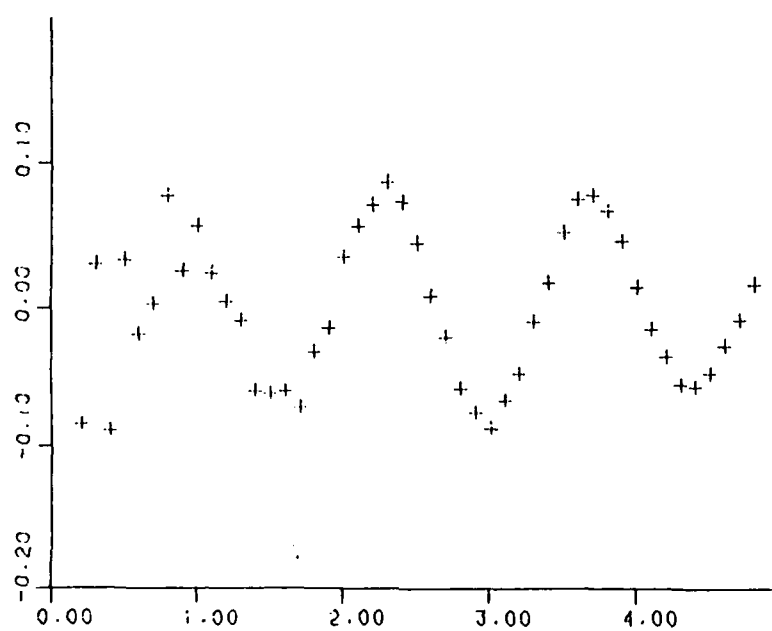


Figure 4.7

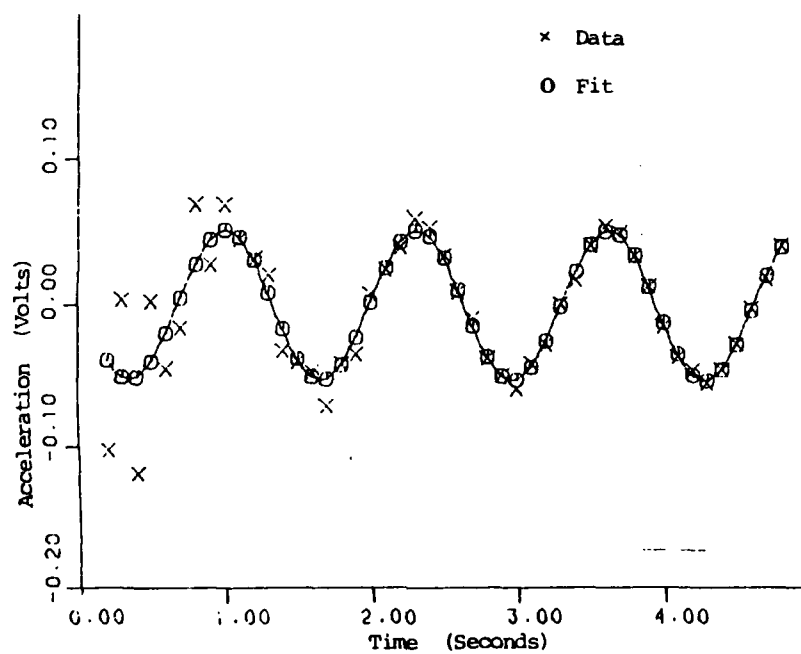


Figure 4.8

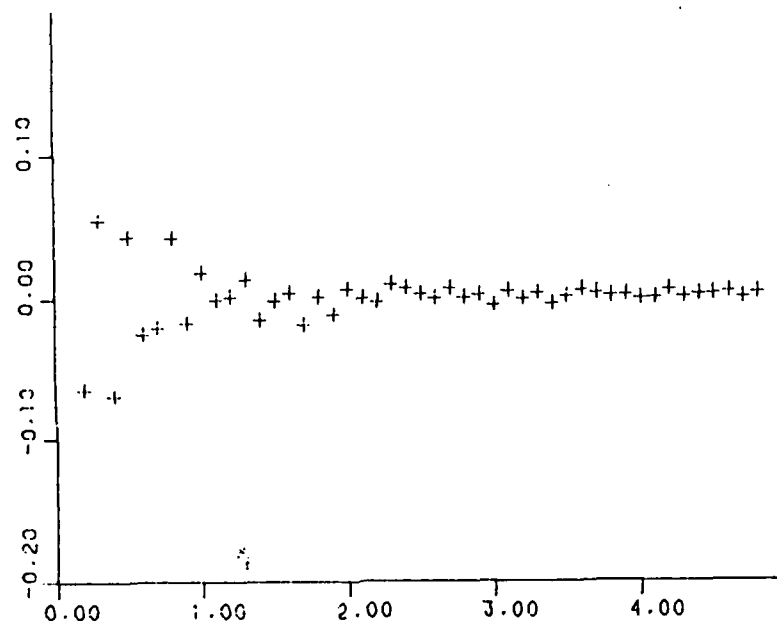


Figure 4.9

In summary, we have seen that analysis of the RPL experimental data can be carried out in several ways with a number of different models. Our techniques can be used to provide reasonable fits of the data to models with or without hose and/or beam damping. Even if one attempts to leave the physics of the hose - beam dynamic interaction unmodeled and perform "model adjustment" (by adjusting the values of the tip mass m_T and beam modulus of elasticity E), our estimation techniques provide a much better fit than that obtained using "modal matching" methods common in engineering practice.

One of the primary objectives of our effort here was to demonstrate the efficacy of our scheme and in particular, to assess its effectiveness when provided with actual experimental data. While we are pleased with the results obtained for the RPL data, we are careful to point out that to provide a fair and complete evaluation of

the usefulness of our models for the RPL experimental structure, a more complete and in-depth study involving extensive experimental work and statistical analysis would necessarily be required.

Acknowledgement The authors would like to thank Dr. Michel A. Floyd of Integrated Systems Inc. in Palo Alto, California for his willingness to discuss the technical details of the RPL structure and for providing us with the experimental data upon which this research was based.

References

- [1] H. T. Banks and J. M. Crowley, Parameter identification in continuum models, J. Astronautical Sciences, 33 (1985), pp.85-94.
- [2] H. T. Banks, J.M. Crowley and I. G. Rosen, Methods for the identification of material parameters in distributed models for flexible structures, ICASE Report No. 84-66, Institute for Computer Applications in Science and Engineering, NASA Langley Research Center, Hampton, VA, 1984, Mat. Aplicada e Computacional, to appear.
- [3] H. T. Banks and I. G. Rosen, A Galerkin method for the estimation of parameters in hybrid systems governing the vibration of flexible beams with tip bodies, ICASE Report No. 85-7, Institute for Computer Applications in Science and Engineering, NASA Langley Research Center, Hampton, VA, 1985.
- [4] H. T. Banks and I. G. Rosen, Computational methods for the identification of spatially varying stiffness and damping in beams, ICASE Report No. 86- , Institute for Computer Applications in Science and Engineering, NASA Langley Research Center, Hampton, VA, 1986.
- [5] R. W. Clough and J. Penzien, Dynamics of Structures, McGraw-Hill, New York, 1975.
- [6] M. A. Floyd, Single-step optimal control of Large Space Structures, Ph.D. Thesis, Department of Aeronautics and Astronautics, Massachusetts Institute of Technology, Cambridge, MA, 1984 and Report CSDL-T-840, The Charles Stark Draper Laboratory, Cambridge, MA, 1984.
- [7] A. Friedman, Partial Differential Equations of Parabolic Type, Prentice Hall, Englewood Cliffs, New Jersey, 1964.
- [8] K. Kunisch and E. Graif, Parameter estimation for the Euler-Bernoulli beam, Mat. Aplicada e Computacional, 4, (1985), pp.95-124.
- [9] J. L. Lions, Optimal Control of Systems Governed by Partial Differential Equations, Springer-Verlag, New York, 1971.
- [10] P. P. Popov, Introduction to Mechanics of Solids, Prentice-Hall, Englewood Cliffs, New Jersey, 1968.
- [11] P. M. Prenter, Splines and Variational Methods, Wiley-Interscience, New York, 1975.

- [12] I. G. Rosen, A numerical scheme for the identification of hybrid systems describing the vibration of flexible beams with tip bodies, J. Math. Anal. Appl., 116, (1986), pp.262-288.
- [13] M. H. Schultz, Spline Analysis, Prentice Hall, Englewood Cliffs, New Jersey, 1973.
- [14] R. E. Showalter, Hilbert Space Methods for Partial Differential Equations, Pitman, London, 1977.
- [15] R. Strunce, et. al., Verification of RCS Controller Methods for Flexible Spacecraft (RPL-EXP), Report CSDL-P-1653, The Charles Stark Draper Laboratory, Cambridge, MA, 1982.

END

1-87

DTIC